AIAA 82-4030

Similarity in Ventilated Wall Jets

R. M. El-Taher*
King Abdulaziz University, Jeddah, Saudi Arabia

A detailed experimental study of a plane jet issuing in the neighborhood of a plane parallel wall is described. Measurements are made for wall static pressures, mean velocity, longitudinal turbulent velocity, transverse turbulent velocity, and Reynolds shear stress. These measurements showed that the jet can be divided into the initial merging, the positive pressure gradient, the negative pressure gradient, and the fully developed zones. Within the last three zones similarities of mean velocity, longitudinal turbulent velocity, transverse turbulent velocity, and Reynolds shear stress have been found.

Nomenclature

b = jet length scale (see Fig. 1)
h = jet offset distance
p = static pressure
p_a = atmospheric pressure
R = Reynolds number ($=U_0 t/\nu$)
t = width of jet nozzle
U = mean velocity in x direction
U_0 = mean velocity at nozzle exit
U_m = local maximum value of U
u' = fluctuating component of velocity in x direction
v' = fluctuating component of velocity in y direction
x = coordinate parallel to wall
y = coordinate normal to wall
$y_{1/2}$ = coordinate of point in the inner region where the velocity is $\frac{1}{2}U_m$
δ = y value where maximum mean velocity occurs
$\bar{\delta}$ = coordinate of the point of zero shear
ρ = density
τ = wall shear stress
ν = kinematic viscosity

Subscripts

m_i = maximum value in the inner region
m_o = maximum value in the outer region
S = secondary flow

Introduction

IF a two-dimensional jet issuing from a nozzle is brought near a flat wall placed parallel and offset to the jet axis, a pressure difference is produced between the outer side of the jet and the wall. This pressure difference causes the jet to deflect toward the wall and flow along it. If there is no opening between the jet and the wall, a step-like flow exists and a recirculating flow region is formed near the nozzle outlet. This type of flow has been studied by many investigators.[1-6]

In many practical applications, an opening exists between the jet and the wall. A secondary flow is entrained through the opening and prevents the formation of a recirculation region. These situations may be encountered in powered high-lift systems of aircraft and in boundary-layer control devices. Marsters[7,8] has denoted this arrangement by the term "ventilated jet."

Marsters[7,8] experimentally investigated the attachment of a ventilated plane jet to parallel and inclined plane walls. His work was concerned mainly with wall static pressures and mean velocity profiles. In studying similarity of mean velocity profiles Marsters divided the flowfield into two regions. These are before and after the point of maximum wall static pressure.

The purpose of the present investigation is to obtain information about the mean flowfield as well as the turbulence characteristics of a ventilated plane jet attached to a parallel wall. The investigation is concerned with the case in which the ratio between the jet offset distance and the nozzle slot width h/t is relatively small. Turbulence measurements included longitudinal turbulence velocity u', lateral turbulence velocity v', and the Reynolds shear stress $\overline{u'v'}$. The similarities of mean velocity and turbulence quantities are also investigated.

From the wall static pressure distribution, the similarity curves of U, $\sqrt{\bar{u}'^2}$, $\sqrt{\bar{v}'^2}$, and $\overline{u'v'}$, the ventilated wall jet can be separated into the initial merging, positive pressure gradient, negative pressure gradient, and fully developed zones. These four zones are shown in Fig. 1. The initial merging zone starts at the nozzle exit and ends roughly at the plane where the potential core disappears. The initial merging zone consists of the potential core, the outer mixing region, and the inner mixing region. The outer mixing region is that where the flow is similar to a free boundary jet problem, while the inner mixing region is where mixing between the main jet and the entrained secondary flow takes place.

The initial merging zone is followed by the positive pressure gradient zone which is characterized by a wall static pressure of positive gradient. This zone can be subdivided into an outer region (a free mixing region) and an inner region (a class of confined plane jet with no circulation). This zone ends at the point of maximum wall static pressure. The negative pressure gradient zone follows the positive gradient zone and ends at the location where the wall static pressure is atmospheric. It can also be subdivided into an outer region and an inner region. The wall static pressure in the fully developed flow zone is atmospheric. It starts at the end of the negative pressure gradient zone and extends over the remaining length of the wall.

Similarities of mean velocity U and turbulence quantities $\sqrt{\bar{u}'^2}$, $\sqrt{\bar{v}'^2}$, and $\overline{u'v'}$ in the positive pressure gradient, negative pressure gradient, and fully developed zones are investigated in the present paper. A detailed experimental study of the initial merging zone is given in Ref. 9.

Apparatus

The nozzle block used in the present investigation has a slot 3 mm in width and 150 mm in span. The nozzle is supplied with air from a centrifugal compressor via a throttling valve. The settling space before the slot contains a perforated plate followed by two screens. The contraction ratio of the nozzle is 33/1. The bottom wall of the nozzle is 2 mm thick and it is

Received Jan. 28, 1981; revision received June 16, 1981.

*Associate Professor, Mechanical Engineering Department. Member AIAA.

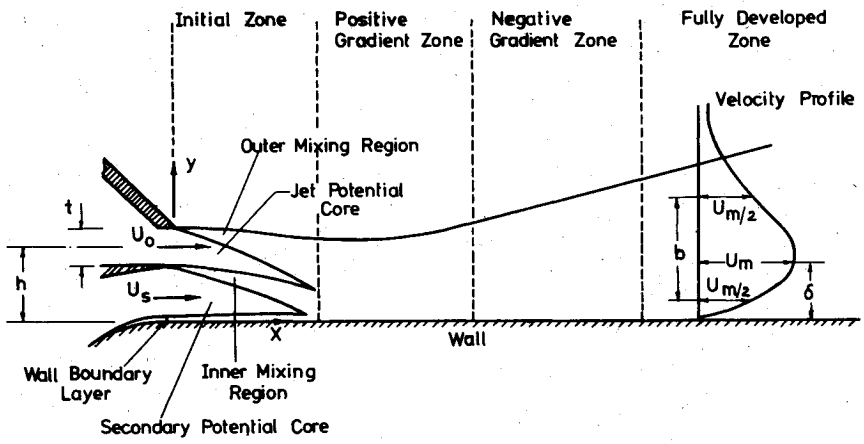

Fig. 1 Schematic profile of ventilated wall jet.

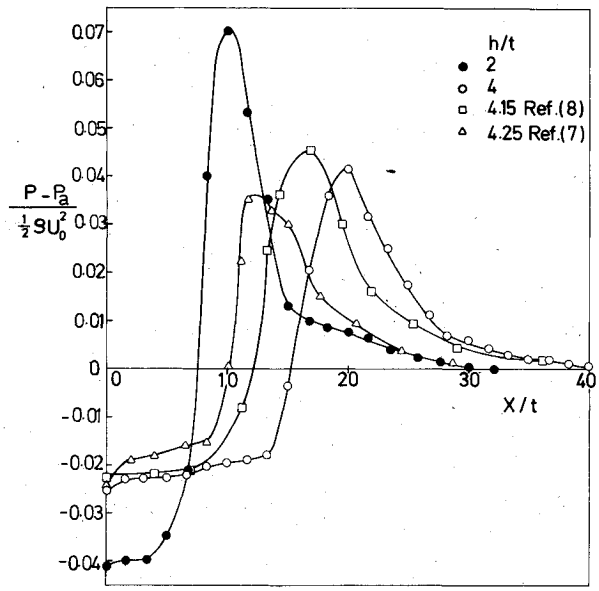

Fig. 2 Wall static pressure distribution.

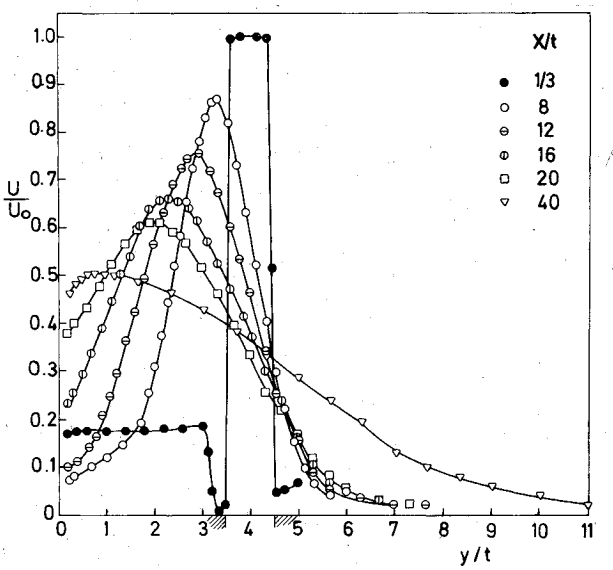

Fig. 3 Mean velocity distribution ($h/t=4$).

chamfered at the exit as shown in Fig. 1. The plane wall was made of a Perspex plastic sheet 6 mm thick. The leading edge of the plane wall is semicircular with a radius of 12 mm. The total length of the plane wall is 450 mm and it is equipped with 0.5 mm diam pressure taps 5 mm apart along the wall centerline. The wall-to-slot offset distance h can be changed by using gage blocks. The nozzle block and the plane wall are mounted between two parallel confining side walls. The side walls were large enough to completely prevent inflow from the sides to produce satisfactory two-dimensional flow. A traversing mechanism allows hot-wire traverses to be carried out at x stations up to $150t$. Traverses were carried out only at the midplane along a path normal to the plane wall. The mean velocity U and turbulence parameters $\sqrt{\bar{u}'^2}$, $\sqrt{\bar{v}'^2}$, and $\overline{u'v'}$ are measured with a hot-wire anemometer of a constant-temperature type with a linearized output. A miniature X probe was used. The probe was made of platinum-plated tungsten wire of 5×10^{-6} m diam with a wire length of about 1 mm. The probe is calibrated before and after each run to check for the repeatability of the calibration.

Measurements were performed for nozzle mouth velocity of 60 m/s which corresponds to an exit Reynolds number ($R=U_0t/\nu$) of 1.48×10^4. With the flow issuing as a free jet, the velocities at the nozzle outlet section were uniform over 85% of the slot width. Spanwise velocity distribution at the nozzle outlet section was found to be highly uniform. The turbulence level at the nozzle outlet was 0.22%. Detailed measurements were performed for two jet offset distances: $h/t=2$ and $h/t=4$.

Results and Discussions

Wall Static Pressure

Figure 2 shows the wall static pressure distribution for $h/t=2$ and 4. It is noticed that the wall static pressure distribution can be divided into four distinct zones: 1) a zone of constant subatmospheric pressure starting at the nozzle slot, 2) a zone with positive pressure gradient, 3) a zone of negative pressure gradient starting at the maximum pressure point and ending where the pressure is atmospheric, and 4) a zone with constant atmospheric pressure extending over the remaining part of the wall. It is remarkable that the magnitude of wall pressures corresponding to $h/t=2$ are larger than those corresponding to $h/t=4$. However, the minimum subatmospheric gage pressure for $h/t=2$ is only 4% of the nozzle exit dynamic pressure and the maximum surface gage pressure is 7% of the nozzle exit dynamic pressure. Figure 3 also shows Marster's results[7,8] for $h/t=4.15$ and 4.25. The differences between the present results and Marster's results are due to different shapes of the parallel wall leading edges used in the different experiments.

Mean Velocity

The mean velocity profiles at different x stations for $h/t=4$ are shown in Fig. 3. The velocity profile at $x/t=\frac{1}{3}$ indicates

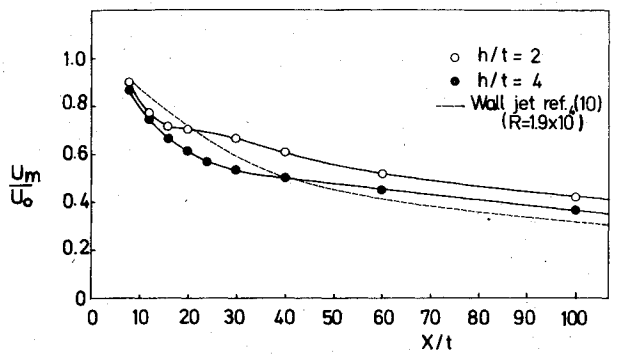

Fig. 4 Decay of maximum jet velocity.

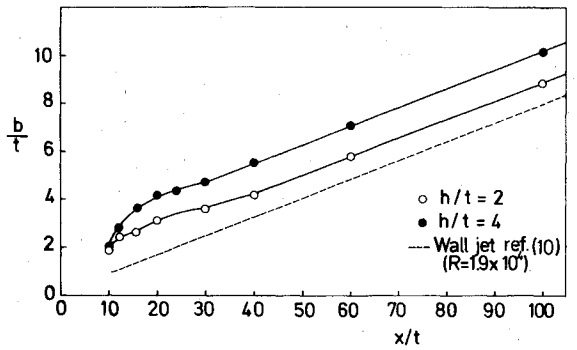

Fig. 5 Growth of jet length scale.

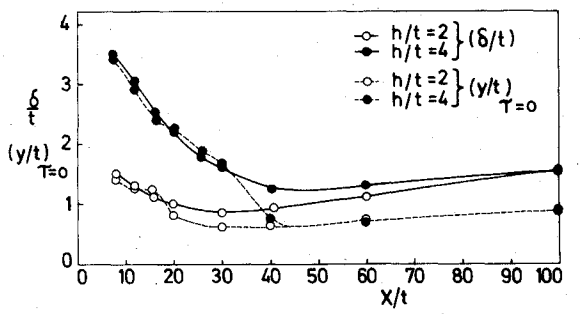

Fig. 6 Locations of maximum velocity and zero shear.

that a secondary entrained flow of relatively uniform velocity over the gap width exists. The figure shows that the ratio U_s/U_0 for $h/t=4$ is 0.17. However, the corresponding ratio for $h/t=2$ was found to be 0.24. The wake of the lower plate of the nozzle is readily noticeable in the velocity profile at $x/t=⅓$. The decay of maximum jet velocity with increasing downstream distance is shown in Fig. 4. Also, the figure shows the decay of maximum velocity of a wall jet as given in Ref. 10. The maximum jet velocity at any streamwise location for $h/t=2$ is larger than the corresponding value for $h/t=4$. In the fully developed zone, the maximum velocity in both cases of ventilated wall jets is larger than the corresponding velocity in the case of wall jet without ventilation as given in Ref. 10. However, the rate of decay in the three cases is the same. Figure 5 shows the growth of jet width with increasing downstream distance. It is found that at any distance x the jet width for $h/t=4$ is larger than the corresponding width for $h/t=2$. This is expected, because increasing the wall offset spreads the jet in the transverse direction more than the smaller offset. For this reason the jet width in each case of the ventilated jet is larger than the width of the normal wall jet. The large jet width corresponding to $h/t=4$ is accompanied by a small value of U_m/U_0 as can be seen from Fig. 4. As

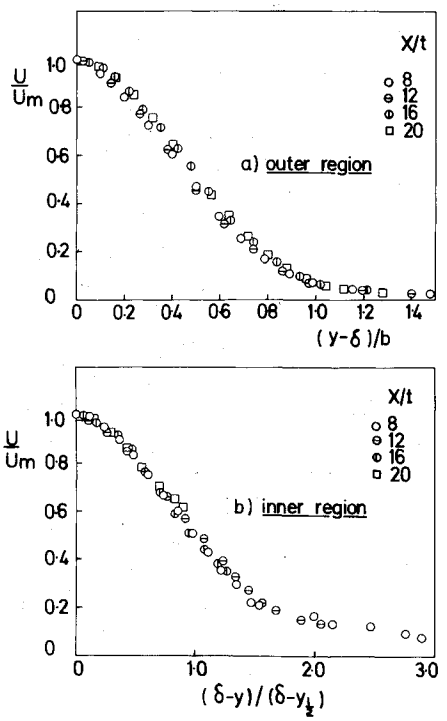

Fig. 7 Similarity of mean velocity in positive pressure gradient zone ($h/t=4$).

depicted in Fig. 5, one may conclude that in the fully developed zone ($x/t>40$) both the ventilated and normal wall jets have the same rate of width growth with downstream distance.

Figure 6 shows the locations of zero shear stress point together with the locations of maximum mean velocity point. The figure shows that the two points do not coincide. The point of maximum velocity is higher than the zero shear stress point in the positive pressure gradient zone. On the other hand, the opposite is true in the negative pressure gradient zone. However, the shift between the locations of the two points in the two regions is relatively small compared to the shift in the fully developed zone. In the last zone, the zero shear stress point is closer to the wall than the maximum mean velocity point. It is remarkable that the zero shear stress points for $h/t=2$ and 4 coincide in the fully developed zone. Likewise, the points of maximum mean velocity for $h/t=2$ and 4 coincide in the fully developed zone. However, the points of zero shear stress coincide earlier than the points of maximum mean velocity. It is remarkable that the point of minimum value of δ for $h/t=4$ occurs at $x/t=45$ which is the beginning of the fully developed (constant pressure) zone. Likewise, the point of minimum value of δ for $h/t=2$ occurs at $x/t=32$ which is the beginning of the constant pressure zone.

Similarity curves for the outer and inner mixing regions of the positive gradient zone ($8<x/t<20$) are shown in Fig. 7. In Fig. 7a the nondimensional mean velocity ratio U/U_m is plotted against the nondimensional distance $(y-\delta)/b$. In Fig. 7b the nondimensional velocity ratio U/U_m is plotted against the nondimensional distance $(\delta-y)/(\delta-y_{½})$.

Similarity of local mean velocity ratio U/U_m in the negative pressure gradient zone ($22<x/t<26$) was also found in both the inner and the outer regions. The nondimensional distance $(y-\delta)/b$ was suitable for similarity in the outer region. However, in the inner region the suitable nondimensional length was found to be $(\delta-y)/b$. A slight deviation from the similarity curve occurred at $x/t=28$. This deviation increased at $x/t=30$. As can be seen from Fig. 2, the pressure gradient at these two values of x/t is quite different from the gradient in the similarity range $22<x/t<28$.

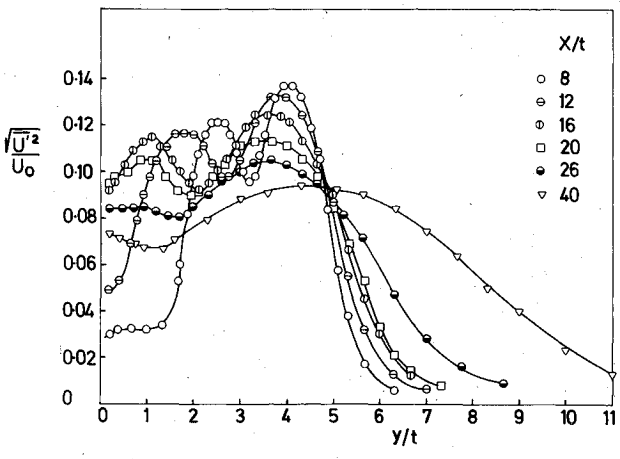

Fig. 8 Distribution of longitudinal turbulent velocity ($h/t=4$).

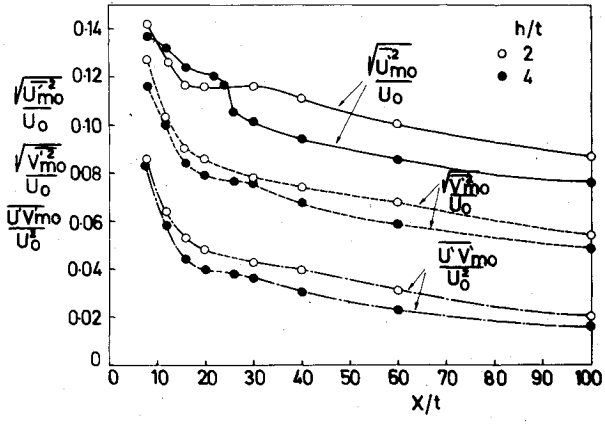

Fig. 9 Distribution of maximum longitudinal turbulent velocity, maximum lateral turbulent velocity, and maximum shear stress in the outer region.

Good similarity of U/U_m against $(y-\delta)/b$ was found in the outer region of the fully developed zone ($x/t>40$). Good similarity in the inner region of that zone was obtained when U/U_m was plotted against y/δ.

Longitudinal Turbulent Velocity

The longitudinal turbulent velocity profiles at different x stations for $h/t=4$ are shown in Fig. 8. It is found that for $x/t<40$ each profile has one peak in both the outer and inner regions. The peak in the outer region is larger than that in the inner region. As can be seen from Fig. 8, the width of the outer region increases with increasing x/t while the width of the inner region decreases by increasing x/t. While the peak in the inner region is appreciably shifted toward the wall with increasing x/t, the shift of the outer peak is relatively small. It is found that the peak in the inner region decreases and moves toward the wall until it finally disappears at $x/t=26$. Comparing Figs. 3 and 8, it is concluded that at $x/t<40$ the minimum value of $\sqrt{\bar{u}'^2}/U_0$ lies at the point of maximum mean velocity.

The distribution of maximum longitudinal turbulent velocity in the outer region is shown in Fig. 9 for $x/t=2$ and 4. In the positive and negative pressure gradient zones, the maximum longitudinal turbulent velocity for $h/t=4$ is larger than that corresponding to $h/t=2$. This indicates that the lower values of longitudinal turbulent velocity corresponds to the steeper pressure gradients. In the fully developed zone, the maximum longitudinal turbulent velocity for $h/t=2$ is larger than the corresponding maximum velocity for $h/t=4$.

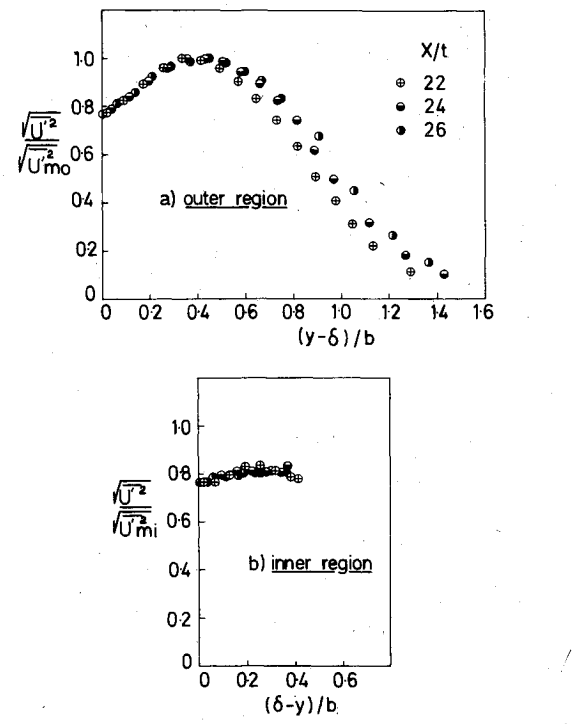

Fig. 10 Similarity of longitudinal turbulent velocity in negative pressure gradient zone ($h/t=4$).

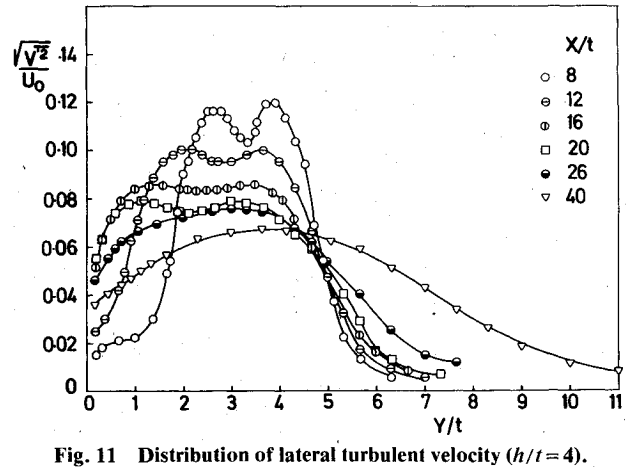

Fig. 11 Distribution of lateral turbulent velocity ($h/t=4$).

Figure 10 shows similarity of longitudinal turbulent velocity in the outer and inner regions of the negative pressure gradient zone. It is remarkable that the longitudinal turbulent velocity in the inner region is constant and equals $0.8\sqrt{\bar{u}'^2_{mo}}$. Similarity in the inner region and in the inner part of the outer region is found to be very good. This is due to the effect of negative pressure at the wall on the mixing process. This effect is not found in the outer part of the outer region where the pressure is atmospheric and consequently there is a deviation in similarity for $(y-\delta)/b>0.5$.

Similarity of the longitudinal turbulent velocity in the outer and inner regions of the positive pressure and fully developed zones was found to be as good as similarity in the negative pressure zone. However, the similarity distance was $(\delta-y)/(\delta-y_{1/2})$ in the inner region of the positive pressure gradient zone and was y/δ in the inner region of the fully developed zone.

Transverse Turbulent Velocity

The distribution of the transverse turbulent velocity at different streamwise stations is shown in Fig. 11. It is found

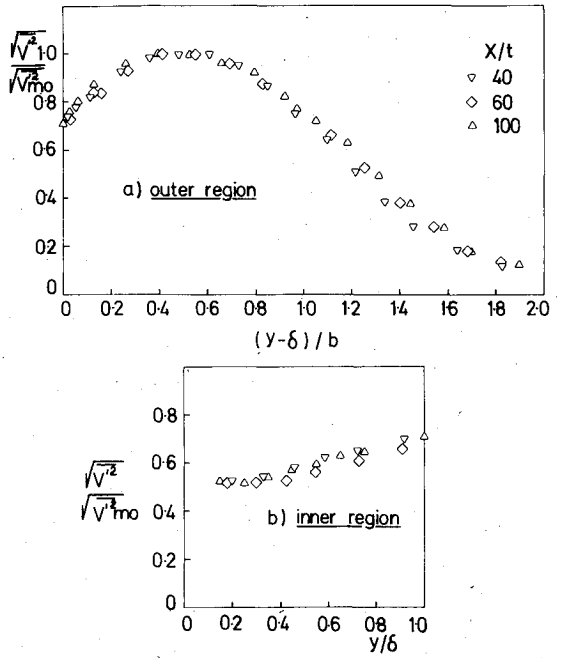

Fig. 12 Similarity of lateral turbulent velocity in fully developed zone ($h/t=4$).

that the peak transverse turbulent velocity in the outer region is equal to the inner regions peak. As can be seen from the figure, the width of the outer region increases with increasing downstream distance. In contrast to that, the width of the inner region decreases with increasing x/t. The peak in the outer and inner regions are shifted toward the plane wall as x increases. The peak of the inner region disappears at $x/t=26$ (the end of the negative pressure gradient zone).

The variation of maximum transverse turbulent velocity in the outer region is shown in Fig. 9. It is found that at any streamwise station, $\sqrt{\bar{v}'^2_{mo}}/U_0$ for $h/t=2$ is larger than the corresponding value for $h/t=4$. The rate of decrease of $\sqrt{\bar{v}'^2_{mo}}/U_0$ with increasing downstream distance is the same for the two cases in the fully developed zone.

Similarity of transverse turbulent velocity profiles in the inner and outer regions of the fully developed zone is shown in Fig. 12. It was found that in the outer region of the positive pressure gradient zone, $\sqrt{\bar{v}'^2}/\sqrt{\bar{v}'^2_{mo}}$ correlates well with the nondimensional distance $(y-\delta)/b$. The correlation in the inner region was good between $\sqrt{\bar{v}'^2}/\sqrt{\bar{v}'^2_{mo}}$ and $(\delta-y)/(\delta-y_{1/2})$. In the outer and inner regions of the negative pressure gradient zone the similarity length scales were found to be $(y-\delta)/b$ and $(\delta-y)/b$, respectively.

Reynolds Shear Stress

Distributions of $\overline{u'v'}/U_0^2$ at different streamwise stations are shown in Fig. 13. The peak of $\overline{u'v'}$ in the outer region is approximately equal to the peak in the inner region. The peaks in the inner and outer regions decrease and shift toward the wall with increasing the downstream distance. The width of the outer region increases with increasing x/t while the width of the inner region decreases. The peak in the inner region disappears at $x/t=40$ (the starting point of the fully developed zone).

The variation of the maximum Reynolds shear stress in the outer region is shown in Fig. 9. It is found that the rate of decrease of $\overline{u'v'_{mo}}$ in the positive pressure gradient zone is larger than the rate in the other two zones. It is found also that Reynolds shear stress for $h/t=2$ is larger than its value for $h/t=4$. However, the rate of decrease of $\overline{u'v'_{mo}}$ in the fully developed zone is the same in both cases.

Similarity of Reynolds shear stress in the positive pressure gradient zone is shown in Fig. 14. In the outer region the ratio

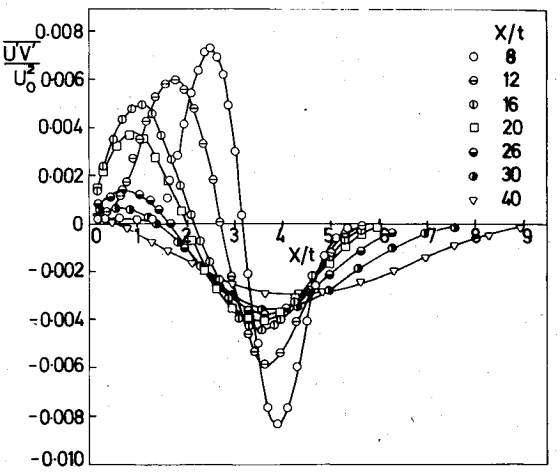

Fig. 13 Distribution of shear stress ($h/t=4$).

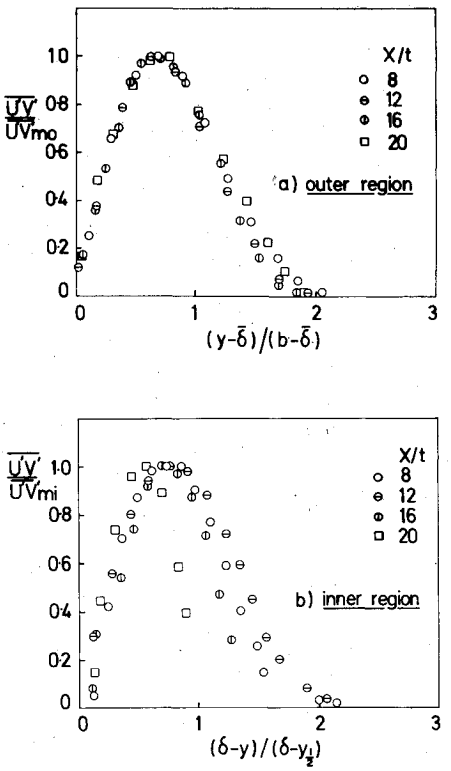

Fig. 14 Similarity of shear stress in positive pressure gradient zone ($h/t=4$).

$\overline{u'v'}/\overline{u'v'_{mo}}$ is plotted against $(y-\delta)/(b-\delta)$. Similarity of Reynolds shear stress profiles against the nondimensional distance $(y-\delta)/b$ has been found to be not as good as that presented in Fig. 14a. The Reynolds shear stress profile corresponding to $x/t=20$ deviates appreciably from the similarity curve in the inner region. This deviation was also noticed in the similarity curve of the transverse turbulent velocity. The deviation in both cases is due to the location of the point $x/t=20$ on the border between the positive pressure gradient zone and the negative pressure gradient zone.

Experimental results showed good similarity of Reynolds shear stress in the inner and outer regions of both the negative pressure gradient zone and fully developed zone. The similarity length variables mentioned above in correlating $\sqrt{\bar{u}'^2}$ and $\sqrt{\bar{v}'^2}$ in both zones were found suitable for correlating the Reynolds shear stress.

Conclusions

Measurements of wall static pressure, mean velocity, longitudinal turbulent velocity, transverse turbulent velocity, and Reynolds shear stress in the ventilated wall jet of relatively small gap-to-slot ratio permit the isolation of four separate zones: the initial merging, the positive pressure gradient, the negative pressure gradient, and the fully developed zones. The streamwise extent of the different zones depends on the jet gap-to-slot ratio h/t. The initial merging zone starts at the nozzle exit and ends roughly at the plane where the potential core disappears. The initial merging zone is followed by the positive pressure gradient zone which is characterized by a wall static pressure of positive gradient. The outer region of the positive pressure gradient zone is a free mixing region. The inner region is a class of confined jet with no circulation. The negative pressure gradient zone starts at the maximum pressure point and ends at the location where the wall static pressure is atmospheric. The negative pressure gradient zone is followed by the fully developed zone in which the wall static pressure is atmospheric.

Similarity of mean velocity, longitudinal turbulent velocity, transverse turbulent velocity, and Reynolds shear stress profiles has been found in the inner and outer regions of the positive gradient, negative gradient, and fully developed zones. The dimensionless quantity $(y-\delta)/b$ is found suitable in representing the similarity profiles of the mean velocity and the turbulence quantities $\sqrt{\bar{u}'^2}$, $\sqrt{\bar{v}'^2}$, and $\overline{u'v'}$ in the outer region of each of the three zones. However, it is found that similarity in the inner region requires a different non-dimensional coordinate for each zone.

References

[1] Bourque, C. and Newman, B. G., "Reattachment of a Two-Dimensional Incompressible Jet to an Adjacent Flat Plate," *Aeronautical Quarterly*, Vol. XI, 1960, pp. 201-232.

[2] Sawyer, R. A., "Two-Dimensional Reattaching Jet Flows Including the Effect of Curvature on Entrainment," *Journal of Fluid Mechanics*, Vol. 17, 1963, pp. 481-498.

[3] Bourque, C., "Reattachment of a Two-Dimensional Jet to an Adjacent Flat Plate," *Advances in Fluidics*, edited by Forbes T. Brown, ASME, New York, 1967.

[4] Kumada, M., Mabuchi, I., and Oyakawa, K., "Studies in Heat Transfer to Turbulent Jets with Adjacent Boundaries," 3rd Rept., *Bulletin of Japanese Society of Mechanical Engineers*, Vol. 16, 1973, pp. 1712-1722.

[5] Ayukawa, K. and Shakouchi, T., "Analysis of a Jet Attaching to an Offset Parallel Plate," *Bulletin of Japanese Society of Mechanical Engineers*, Vol. 19, 1976, pp. 395-401.

[6] Parameswaran, V. and Alpay, S. A., "Studies on Reattaching Wall Jets," *Transactions of Canadian Society of Mechanical Engineers*, Vol. 3, 1975, pp. 83-94.

[7] Marsters, G. F., "The Attachment of a Plane Ventilated Jet to a Plane Parallel Wall," *Transactions of Canadian Society of Mechanical Engineers*, Vol. 4, No. 4, 1976-77.

[8] Marsters, G. F., "The Attachment of a Ventilated Plane Jet to an Inclined Plane Wall," *Aeronautical Quarterly*, Vol. 29, May 1978, pp. 60-72.

[9] El-Taher, R. M., "Experimental Study of the Flow Field Near the Nozzle in Ventilated Wall Jet," to be published in *Journal of Engineering and Applied Sciences*, Vol. 1, No. 3, 1982.

[10] Myers, G. E., Schauer, J. J., and Eustis, R. H., "The Plane Turbulent Wall Jet," Dept. of Mechanical Engineering, Stanford University, Stanford, Calif., Tech. Rept. 1, 1961.